Surface electronic structure and chemisorption on corundum transition-metal oxides: α-Fe_2O_3

Richard L. Kurtz* and Victor E. Henrich
Applied Physics, Yale University, New Haven, Connecticut 06520
(Received 22 January 1987)

Ultraviolet photoemission spectroscopy has been used to study the electronic structure of both nearly stoichiometric, well-ordered α-Fe_2O_3 surfaces and surfaces containing point defects. The interaction of O_2, H_2O, H_2, and SO_2 with both types of surfaces has also been investigated. The energy levels of the five $3d$ electrons on the Fe^{3+} ions overlap those of the filled O $2p$ orbitals, leading to a complex valence band about 10 eV wide. Oxygen-vacancy surface defects produced by Ar^+-ion bombardment result in a conducting surface layer containing both Fe^{2+} and Fe^0 ions. The well-ordered α-Fe_2O_3(0001) surface is relatively inert with respect to all four molecules studied, with exposures greater than 10^3 L (1 L$\equiv 10^{-6}$ Torr sec) necessary before any chemisorption could be seen. For large exposures, the O_2-surface interaction gives rise to a negative adsorbed species. H_2O adsorbs dissociatively on both well-ordered and defect surfaces, resulting in adsorbed OH^- ions. SO_2 appears to bond primarily to surface oxygen ions, yielding a complex similar to SO_4^{2-}.

I. INTRODUCTION

Within the important group of $3d$ transition-metal oxides, those having the trigonal corundum crystal structure are particularly interesting. We have initated a research program to study the surface properties of single-crystal corundum transition-metal oxides, and previous papers have presented the results of measurements of surface electronic structure, the properties of surface defects, and chemisorption on Ti_2O_3 and V_2O_3.[1-6] In this paper we report studies of the surface properties of a third, very important oxide, α-Fe_2O_3, which occurs naturally as the mineral hematite. α-Fe_2O_3 is an antiferromagnetic insulator, and it is fairly active and selective for a number of heterogeneous catalytic reactions. It has also shown promise as a photocatalytic electrode for the production of H_2 from H_2O by means of photoelectrolysis.[7] α-Fe_2O_3 supported on noble metals has also been found to exhibit strong metal-support interactions.[8]

Both Ti_2O_3 and V_2O_3 cleave along the same $(10\bar{1}2)$ crystal plane, and the studies of those materials have been performed on $(10\bar{1}2)$ surfaces cleaved in ultrahigh vacuum (UHV).[1-3,5] However, we have not been able to cleave α-Fe_2O_3 along the same plane, and the small amount of single-crystal material available has necessitated the use of alternative surface preparation procedures. Methods of preparing a (0001) natural growth face of α-Fe_2O_3 were examined and have been published previously.[9] In this paper the surfaces characterized in Ref. 9 will be used to study the valence bands of α-Fe_2O_3 and to investigate its chemisorption properties for a variety of molecules.

Recently Hendewerk *et al.*[10] have reported thermal desorption and photoemission measurements of H_2O adsorption on (001) surfaces of Ge-doped α-Fe_2O_3 prepared in a manner similar to that described previously by Kurtz and Henrich.[9] Their results are in general agreement with the H_2O adsorption results reported here. Fujimori *et al.*[11] have reported synchrotron photoemission and Auger measurements on unspecified α-Fe_2O_3 surfaces that were scraped in vacuum with a diamond file. The resolution in their photoemission spectra was lower ($\sim$0.5 eV) than that in the other studies of α-Fe_2O_3 surfaces.

The experimental techniques used will be discussed briefly in Sec. II. Section III will examine the valence-band electronic structure of α-Fe_2O_3 as determined from ultraviolet photoemission (UPS) measurements; the nature of surface defects will also be considered. Sections IV–VII will present UPS results for the interaction of α-Fe_2O_3(0001) surfaces with O_2, H_2O, H_2, and SO_2, respectively. Section VIII discusses the interpretation of those results in terms of surface electronic structure and possible molecule-surface interactions.

II. EXPERIMENTAL METHODS

The single-crystal α-Fe_2O_3 samples used in this work were supplied by J. P. Remeika of AT&T Bell Laboratories; the methods of surface preparation and characterization have been presented in Ref. 9. Defects were produced by means of 500-eV Ar^+-ion bombardment. UPS spectra were excited with either the He I (21.2 eV) or He II (40.8 eV) lines from a microwave discharge lamp or a hollow cathode dc discharge lamp, respectively. Photoelectron spectra were obtained with a double-pass cylindrical mirror spectrometer operated in the retarding mode at a resolution of 240 meV and were corrected for the presence of satellite lines in the discharge. Unless noted, no inelastic electron background corrections have been made to the data presented. The location of the Fermi level E_F was determined from UPS spectra of atomically clean Au. Auger spectra were excited with an electron gun coaxial with the electron spectrometer.

The O_2 used for chemisorption studies was 99.99% pure. The H_2O used was triply distilled, deionized water contained in a glass vial; details of its purification are given in Ref. 2. The H_2 was 99.9995% pure, and the SO_2 was 99.98% pure. All gases were admitted to the vacuum system through copper-gasket-sealed variable leak

valves. The purity of the gases was monitored with a quadrupole mass spectrometer in the UHV chamber.

III. VALENCE-BAND ELECTRONIC STRUCTURE

As described in detail in Ref. 9, the (0001) natural growth face of α-Fe_2O_3 was prepared by ion bombardment and subsequent annealing in UHV. For annealing temperatures near 700 °C, low-energy electron diffraction (LEED) patterns exhibited both $p(2\times2)$ and $(\sqrt{3}\times\sqrt{3})R30°$ surface reconstructions; annealing to 820 °C or above produced an incommensurate overlayer having the same symmetry as the substrate but a lattice constant differing by 11:12 (or 12:11). X-ray photoelectron (XPS) spectra showed that the surface that had been annealed at 820 °C had a stoichiometry closest to that of bulk Fe_2O_3. In this paper we will thus consider only surfaces annealed to 820 °C and high-defect-density ion-bombarded surfaces.

The He I UPS spectrum for ion-bombarded α-Fe_2O_3(0001) is shown in Fig. 1(a), that for the 820 °C-annealed surface is shown in Fig. 1(b), and the He II UPS spectrum for the annealed surface is shown in Fig. 1(c). The electronic configuration of the cations in α-Fe_2O_3 is $3d^5$, with the five $3d$ orbitals overlapping the O $2p$ contribution to the valence band. This gives rise to a rather complicated structure for the valence band even in the semi-angle-integrated UPS spectra shown here. In order to get some idea of the origin of the various features in these spectra, we have decomposed them into a sum of Gaussian peaks, using the minimum number necessary to reproduce the major features in the spectra. Six Gaussians are adequate to fit the observed spectra, with one being very small and only necessary to fit the very bottom of the valence band near 10 eV below E_F; a respectable fit could have been obtained by using only five Gaussians. Smooth backgrounds, indicated by the long-dashed lines in Fig. 1, were subtracted from the spectra before fitting (see Ref. 2 for a discussion of background subtraction techniques). The sum of the Gaussians and the background function is given by the dotted curve for each spectrum. The Gaussians were constrained to have the same energy locations relative to E_F for all three spectra, but their amplitudes and full widths at half maximum (FWHM's) were independently adjusted to give the best fit. Table I presents the resultant energy locations, widths, and relative intensities of the Gaussians used.

Since there was no physical justification for choosing the parameters of the Gaussians in Fig. 1 other than to adequately describe the UPS spectra, those peaks cannot be identified with specific atomic orbitals of the Fe and O ions. It is instructive, however, to compare the relative amplitudes of the peaks with the stoichiometry of the surface and with the magnitude of the contributions of the various valence states of Fe to the XPS spectra of the Fe $2p$ core levels (see Ref. 9). Such a comparison should at least indicate to what region of the valence band the d orbitals of the various ions contribute. Both XPS and Auger spectra indicate that the ion-bombarded surface is O deficient relative to the 820 °C annealed surfaces and to bulk α-Fe_2O_3. XPS spectra for the ion-bombarded surface also exhibit major contributions from Fe^{2+} cations, with smaller contributions from Fe^{3+} (including the bulk contribution) and metallic Fe^0; the more metallic nature of the ion-bombarded surface is evident in Fig. 1(a) from the relatively large density of states at E_F. The XPS spectra for the 820 °C-annealed surface exhibit no Fe^0 contribution and only a minor Fe^{2+} contribution; the cation electron configuration on this surface is predominantly Fe^{3+}. The changes in stoichiometry upon annealing thus suggest that the peaks in the UPS spectra at 2.8 and 4.1 eV below E_F are primarily of O origin. The peak at 0.9

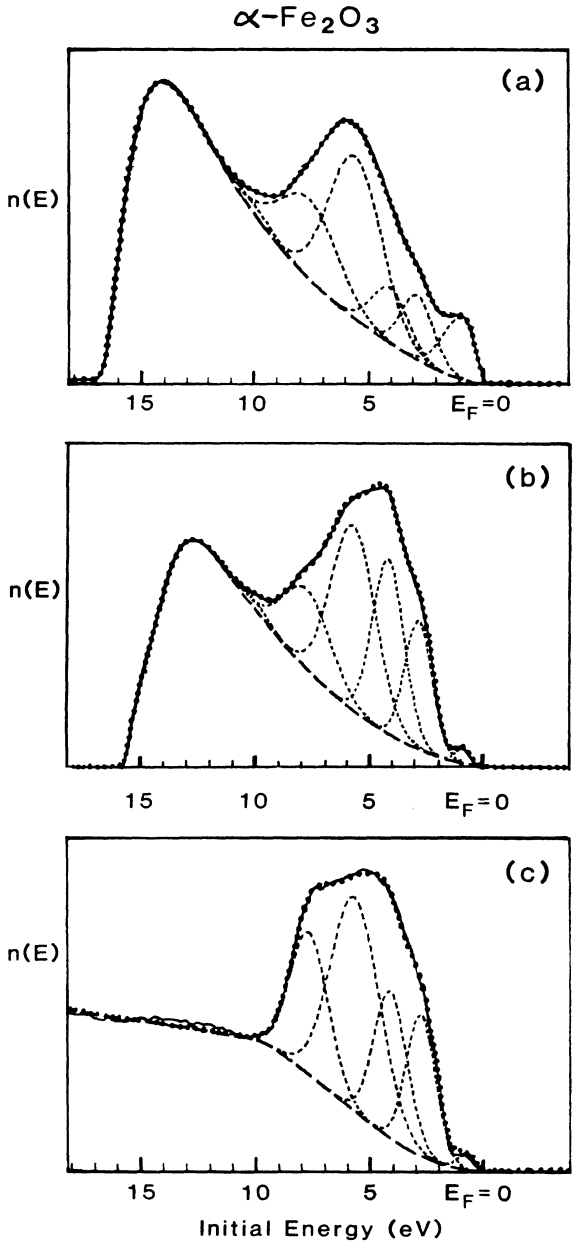

FIG. 1. (a) He I UPS spectrum of Ar^+-ion-bombarded α-Fe_2O_3(0001); (b) He I and (c) He II spectra for ion-bombarded α-Fe_2O_3(0001) annealed at 820 °C.

TABLE I. Energy locations (eV), FWHM's (eV), and areas (percent of total emission intensity) of the Gaussians used in the decomposition of the UPS spectra of α-Fe_2O_3(0001) plotted in Fig. 1.

Surface	Ion bombarded		820 °C-annealed			
$h\nu$	21.2 eV		21.2 eV		40.8 eV	
Energy	FWHM	Area	FWHM	Area	FWHM	Area
0.92	2.00	12	0.70	1	0.80	1
2.79	1.70	10	1.40	16	1.50	6
4.11	1.90	10	1.63	26	1.70	19
5.64	2.75	43	2.30	38	2.55	42
7.67	3.00	23	2.50	18	2.00	22
9.99	1.90	2	1.40	1		0

eV for the ion-bombarded surface, which is responsible for its metallic nature, correlates best with the presence of Fe^0 atoms. However, the residual peak at that energy for the annealed surface is believed to be a cation-derived surface state; this will be discussed in Sec. VIII below. The remaining structure in the valence band is presumably of primarily cation origin.

The work function for the ion-bombarded α-Fe_2O_3(0001) surface, determined from the vacuum level cutoff of inelastically scattered electrons in the He I spectra, is 4.6±0.2 eV. After annealing to 820 °C the work function increases to 5.4±0.2 eV. A similar decrease in work function upon ion bombardment of annealed α-Fe_2O_3 surfaces was observed by Hendewerk *et al.*[10]

The changes that are produced in UPS spectra of the annealed surface as defects are created in a controlled manner by ion bombardment [i.e., proceeding from the surface in Fig. 1(b) to that in Fig. 1(a)] are shown in Fig. 2. The introduction of a low density of defects causes the feature at 0.9 eV to broaden and increase in intensity, while emission from the upper edge of the valence band decreases in intensity, indicating that the O levels near the surface are becoming depopulated, in agreement with the loss of O indicated by the Auger and XPS spectra. As the defect density increases (i.e., longer sputtering times), the peak initially at 0.9 eV becomes a dominant feature in the valence-band spectrum; it has increased an order of magnitude in intensity and almost tripled in width, now overlapping E_F. The overall width of the valence band remains essentially constant upon defect creation, but its shape changes significantly.

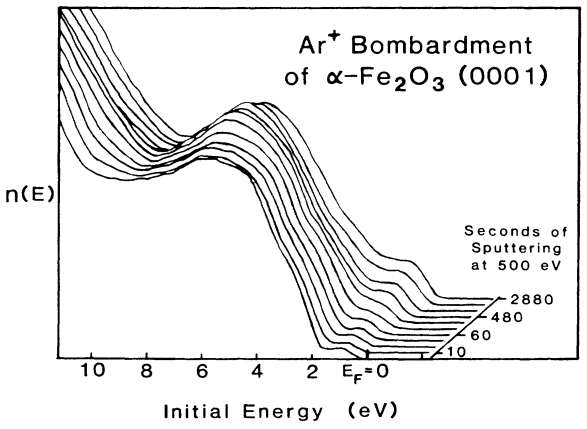

FIG. 2. He I UPS spectra for increasing Ar^+-ion-bombardment time of 820 °C α-Fe_2O_3(0001).

At low densities, surface defects probably consist of isolated O vacancies, although additional atomic rearrangement of the surface following the creation of such a defect is no doubt more important for the (0001) surface of α-Fe_2O_3 than for the $(10\bar{1}2)$ surfaces of Ti_2O_3 and V_2O_3 that have been investigated previously.[1-6] This is due to the threefold O coordination of the surface cations on the (0001) surface [versus fivefold for cations on an $(10\bar{1}2)$ surface]; see Ref. 12 for a comparative discussion of the various surfaces. The removal of an O ion from the idealized (0001) surface, shown in Fig. 1 of Ref. 9, would cause the adjacent surface Fe atom to migrate, perhaps moving to an adjacent threefold O site or settling into the now open fivefold hollow in the layer beneath. The presence of an incommensurate overlayer structure on the 820 °C-annealed (0001) surface, however, whose geometry is not known, mitigates against pursuing such detailed models further. Thus defects on α-Fe_2O_3(0001) are complicated and the details of the atomic rearrangement are not understood.

IV. CHEMISORPTION OF O_2

When the 820 °C-annealed α-Fe_2O_3(0001) surface is exposed to successively larger amounts of O_2, the He I UPS spectra shown in Fig. 3 are obtained; Figs. 3(a) and 3(b) show the same series of spectra viewed from different angles. The raw data for this chemisorption series exhibited a puzzling increase in the total spectral intensity, including the inelastic background, for exposures of 10^4 Langmuirs (1 L≡10^{-6} Torr sec) and up; the total intensity increased to more than twice that for the annealed surface. A similar effect has been seen during O_2 exposure of V_2O_3 surfaces,[3] but not for other transition-metal oxides studied in the same UHV surface-analysis system. We have not been able to determine any instrumental cause for this effect. We have, however, removed the effect from the data in Fig. 3 by normalizing the spectra for 10^4 L and up to a constant total valence-band intensity above background. Since this may be an arbitrary correction, we are restricted to making only relative comparisons of band intensities within a particular spectrum above 10^3 L. This normalization procedure has no effect on the determina-

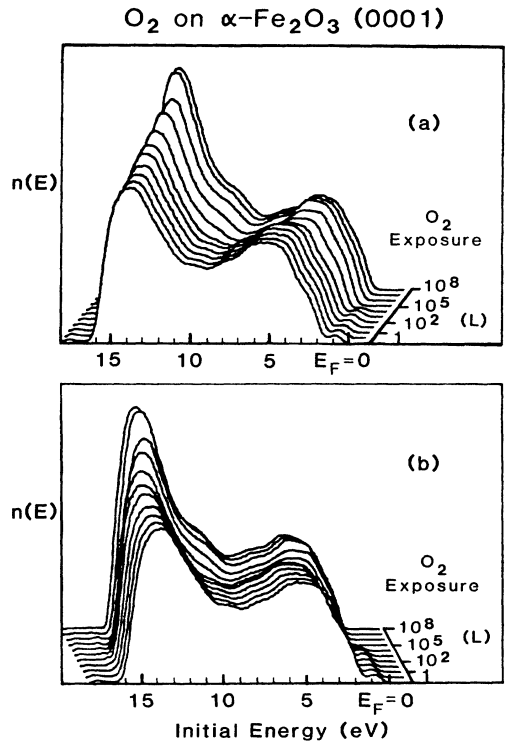

FIG. 3. He I UPS spectra for 820 °C-annealed α-Fe_2O_3(0001) exposed to O_2. The same data are presented in (a) and (b).

tion of work functions or energy locations of features within the bands, however.

The most startling effect seen in Fig. 3 is that there are essentially no changes in the valence-band spectra until the O_2 exposure exceeds 10^3 L. Above 10^3 L, however, the peak at 0.9 eV completely disappears, the upper edge of the valence band moves 0.4 eV closer to E_F, and the work function increases by 0.7 eV. The intensity of the lower part of the valence band (in the region of 6–9 eV) decreases relative to that of the top of the band, although the feature at 10.0 eV grows in relative intensity. Due to the large changes in the valence-band spectra for O_2 exposures above 10^3 L, it is not possible to produce meaningful UPS difference spectra from these data.

When a high-defect-density α-Fe_2O_3(0001) surface is exposed to O_2, the UPS spectra shown in Fig. 4 are obtained. The changes are qualitatively similar to those for annealed surfaces, except that the puzzling increase in overall spectral intensity was not observed. The sputtered surface is much more reactive than the annealed one, exhibiting measureable changes in the UPS spectra after only 0.5 L O_2 exposure. By 100 L O_2 the feature nearest E_F has been reduced in intensity by more than an order of magnitude. It never completely disappears for the defect surface, but after 10^8 L it is barely discernable. The work function increases as the intensity of the peak near E_F decreases, rising by about 0.6 eV after exposures of 10^5–10^8 L O_2. Again the changes produced in the valence-band region by O_2 exposure are too large and complex to permit the use of photoemission difference spectra.

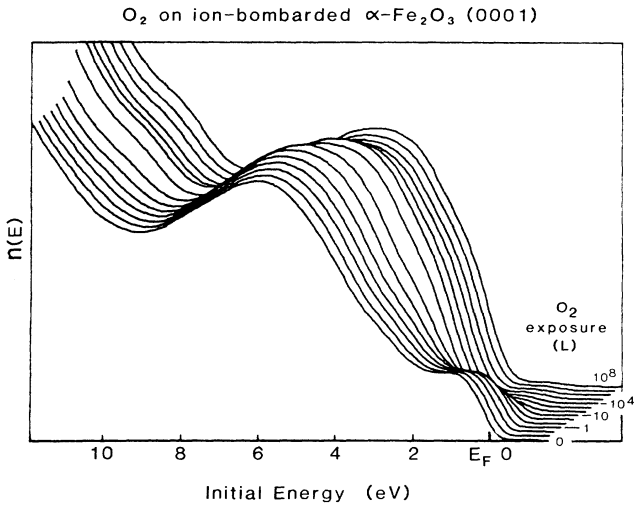

FIG. 4. He I UPS spectra for exposure of Ar^+-ion-bombarded α-Fe_2O_3(0001) to O_2.

V. CHEMISORPTION OF H_2O

The He I UPS spectra that are obtained when the 820 °C-annealed α-Fe_2O_3(0001) surface is exposed to successively larger amounts of H_2O are shown in Fig. 5. The most striking feature of these spectra is that they exhibit very few changes for H_2O exposures below 10^5 L; the only major change is an increase in the background

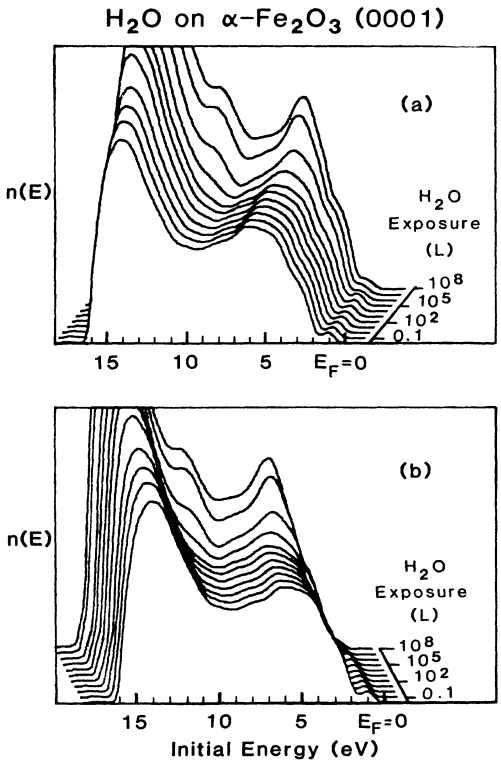

FIG. 5. He I UPS spectra for 820 °C-annealed α-Fe_2O_3(0001) exposed to H_2O. The same data are presented in (a) and (b).

at low kinetic energies. The work function also remains constant up to that exposure. (Hendewerk *et al.*[10] also observed no room-temperature adsorption on stoichiometric surfaces, although their experiments were conducted below 80 L H_2O exposure.) For 10^5 L and above, however, significant changes do occur in the UPS spectra. The sticking coefficient for the adsorbed species on annealed α-Fe_2O_3(0001) is in the range of 10^{-5}–10^{-6}. The change in work function was found to vary from run to run; for the data shown in Fig. 5 it decreased by about 0.4 eV.

In contrast to the case of O_2 chemisorption on this surface, H_2O adsorption does not bend the bands significantly; the upper edge of the valence band remains at the same energy up to the highest exposures. There is also a relatively small interaction between H_2O and the surface state at about 1 eV below E_F. It is possible to produce difference spectra from the data of Fig. 5, and these are plotted in Fig. 6(a). Very little adsorption occurs below 10^5 L, at which point a two-peaked difference spectrum appears. The peaks are located at 5.1 and 10.3 eV below E_F.

More detailed information about the adsorption of H_2O as a function of exposure can be obtained by taking the differences between successive UPS spectra for exposures above 10^3 L; these sequential differences are plotted in Fig. 6(b). The two major peaks at 5.1 and 10.3 eV still dominate these spectra, but there is additional structure near 7.5 and 13 eV; we will return to a discussion of these spectra in Sec. VIII below. Also included in Fig. 6(b) for comparison are the locations of the b_2, a_1, and b_1 molecular orbitals of gas-phase molecular H_2O (Ref. 13) and the 3σ and 1π levels of OH^- in NaOH.[14]

When a high-defect-density α-Fe_2O_3(0001) surface is exposed to H_2O, the He I UPS spectra plotted in Fig. 7(a) are obtained. As for the annealed surface, H_2O does not significantly alter the substrate band structure, so it is possible to produce difference spectra; these are plotted in Fig. 7(b). H_2O interacts with the ion-bombarded surface at much lower exposures than for the annealed surface, with structure in the difference spectra evident below 10 L. These difference spectra also exhibit a two-peaked structure, with the peaks located at 5.2 and 10.3 eV, essentially the same location as for H_2O on annealed α-Fe_2O_3(0001). The work function of the sputtered surface decreases by 0.15 eV during H_2O chemisorption.

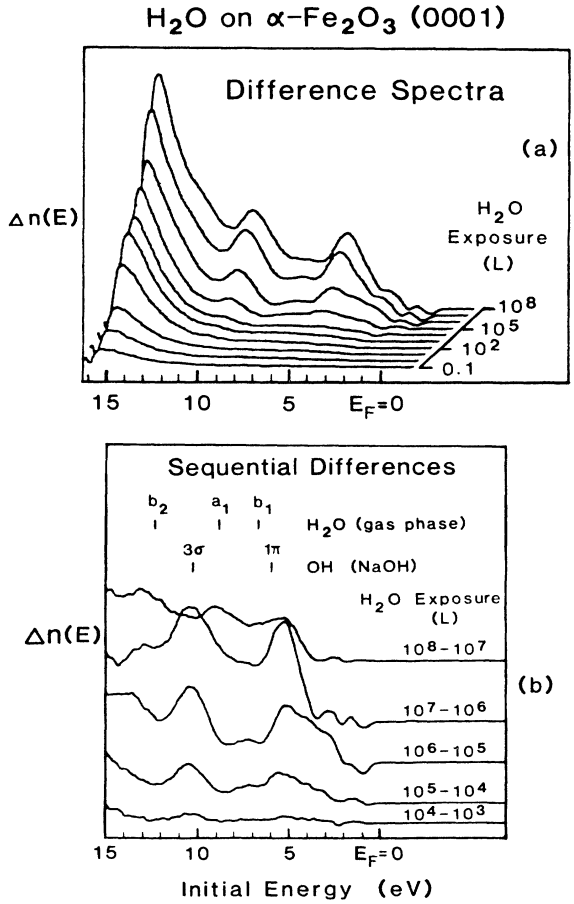

FIG. 6. (a) UPS difference spectra for the data in Fig. 5; (b) sequential difference spectra for the same data.

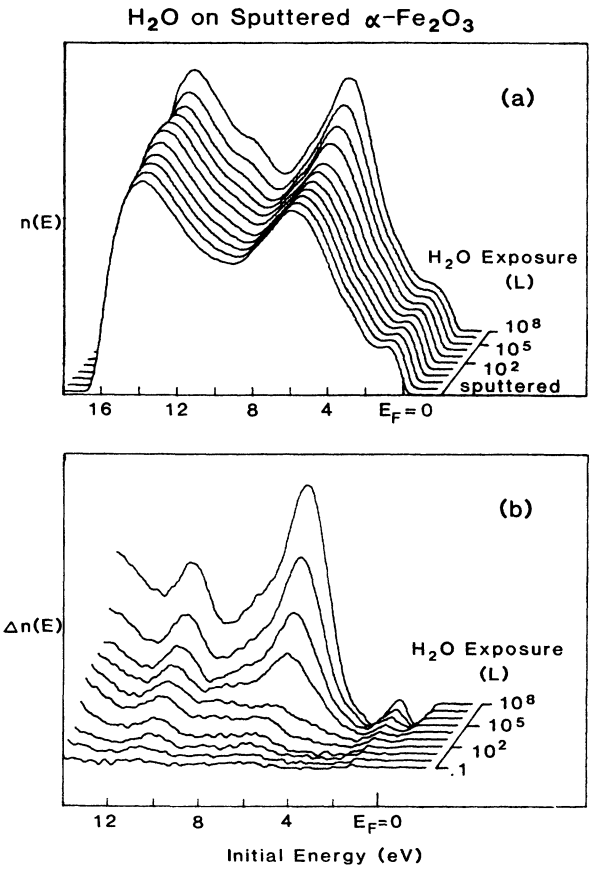

FIG. 7. (a) He I UPS spectra for exposure of Ar^+-ion-bombarded α-Fe_2O_3(0001) to H_2O; (b) UPS difference spectra for the data in (a).

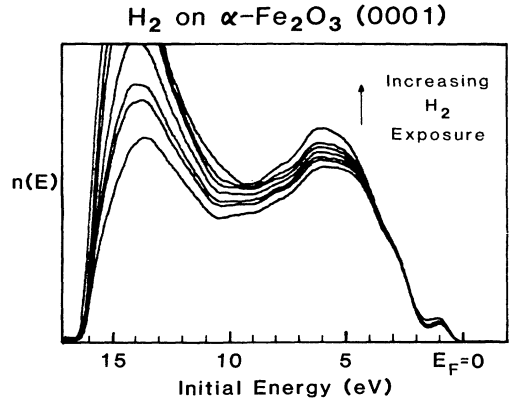

FIG. 8. He I UPS spectra for H_2 exposure of 820 °C-annealed α-Fe_2O_3(0001).

VI. INTERACTION OF α-Fe_2O_3 WITH H_2

Since part of our motivation for studying the surfaces of α-Fe_2O_3 is to investigate its potential for use as an electrode in the photocatalytic production of H_2 from H_2O, we have also investigated the interaction of H_2 with annealed α-Fe_2O_3(0001) surfaces. The 21.2-eV UPS spectra that result from this interaction are presented in Fig. 8 for H_2 exposures of $0.1-10^5$ L. The emission intensity increases in and below the valence-band region with increasing exposure, and at the highest exposures emission in the region of the 0.9-eV peak is also seen to increase. The upper edge of the valence band does not move, and the changes in the valence-band emission are sufficiently small that difference spectra can be produced; these are plotted in Fig. 9(a). In order to better see the changes in the spectra, Fig. 9(b) presents these same differences using an expanded vertical scale after removal of a smooth background from each curve. A broad peak at about 6 eV occurs for low exposures, and a smaller feature at 10.7 eV appears for higher exposures. The work function initially rises slightly, but with the appearance of the 10.7-eV peak it drops to a value 0.1 eV below that for the annealed surface. Also shown in Fig. 9(b) are the locations of the 3σ and 1π levels of OH^- in NaOH.[14]

VII. CHEMISORPTION OF SO_2

Sulfur-containing molecules play a particularly important role in catalysis since they often act as poisons, with the sulfur bonding to active sites on the surface and destroying catalytic activity. When an 820 °C-annealed α-Fe_2O_3(0001) surface is exposed to SO_2, the UPS spectra shown in Fig. 10 are obtained. The change in the work function, $\Delta\phi$, is plotted along the right side of the spectra in Fig. 10(a). This surface is unaffected by SO_2 up to 10^3 L exposure. Above 10^3 L major changes in the UPS spec-

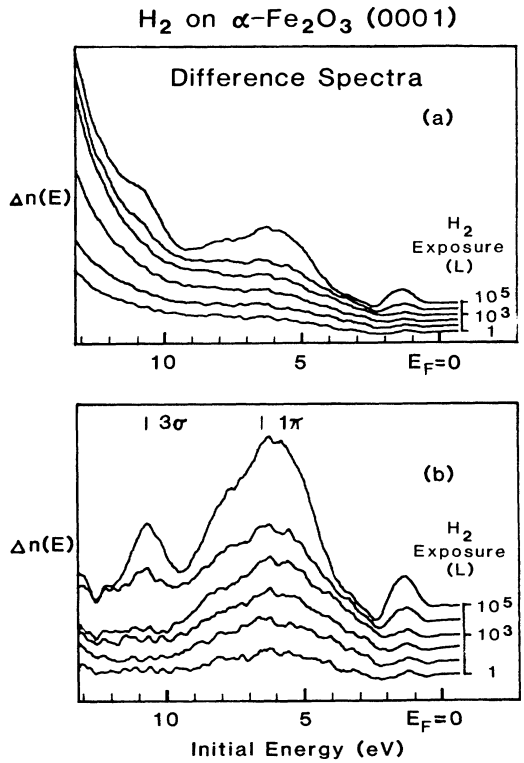

FIG. 9. (a) UPS difference spectra for the data in Fig. 8; (b) the spectra in (a) after removal of a smooth background.

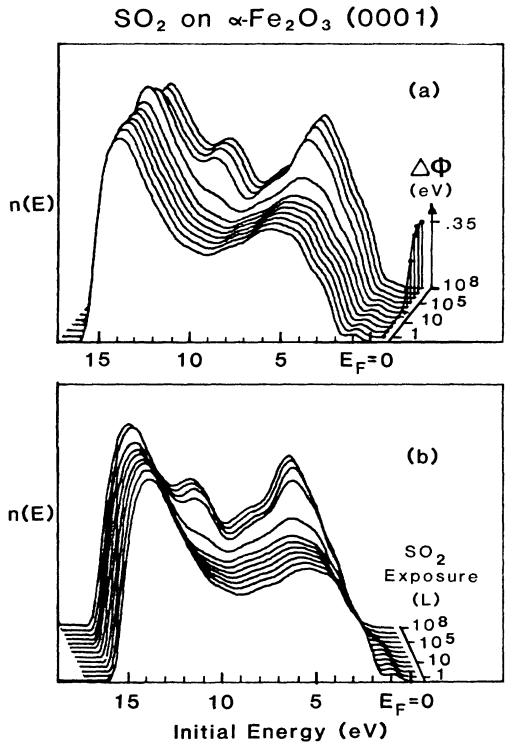

FIG. 10. He I UPS spectra for SO_2 adsorption on 820 °C-annealed α-Fe_2O_3(0001). The same data are presented in (a) and (b). The change in work function, $\Delta\phi$, with exposure is included in (a).

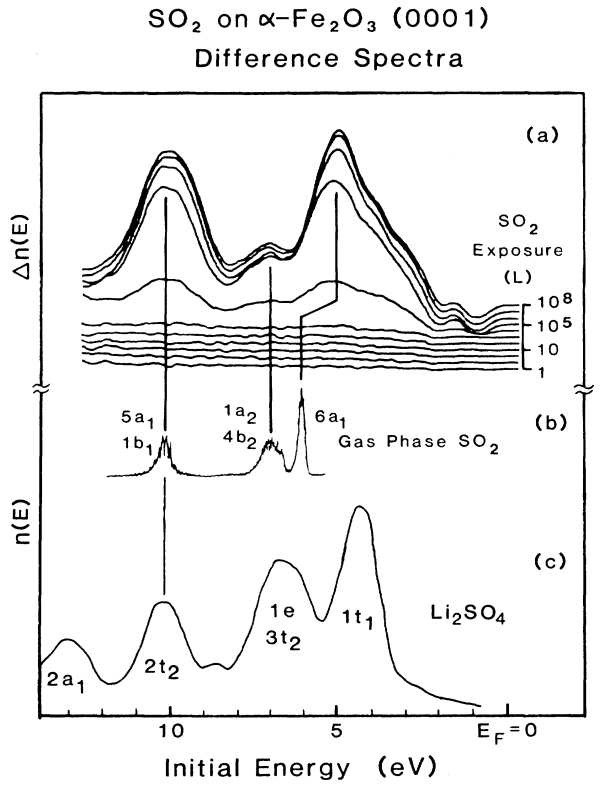

FIG. 11. (a) UPS difference spectra for the data in Fig. 10; (b) He I UPS spectrum of gas-phase SO_2 (from Ref. 11); (c) He II UPS spectrum of SO_4^{2-} in Li_2SO_4 (from Ref. 13).

tra become apparent near 5 and 10 eV below E_F. The 0.9-eV peak is attenuated and the work function increases by 0.35 eV. Since the location of the upper edge of the valence band is unaffected by the presence of the adsorbate, difference spectra can be produced for this chemisorption system; they are plotted in Fig. 11. The difference spectra are dominated by peaks at 5.1 and 10.2 eV, with a third, smaller one at 7.1 eV and a shoulder on the low-binding-energy side of the 5.1-eV peak. The difference spectra show that only one adsorbed phase is present, with a sticking coefficient of roughly 10^{-6}. For comparison, the He I photoelectron spectrum of gas phase SO_2 (Ref. 13) and the He II spectrum of SO_4^{2-} in Li_2SO_4 (Ref. 15) are included in Fig. 11.

VIII. DISCUSSION

A common theme that emerges from the chemisorption experiments discussed above is the inertness of the α-Fe_2O_3(0001) surface. Although the surface used here was not cleaved in vacuum, the XPS studies of various surface preparation procedures described in Ref. 9 indicate that annealing at 820 °C produces a surface whose cations have predominately the Fe^{3+} ($3d^5$) configuration of bulk α-Fe_2O_3. That this half-filled d-band configuration is indeed very stable is confirmed by sticking coefficients of 10^{-4}–10^{-5} for O_2 and H_2, 10^{-5}–10^{-6} for H_2O, and about 10^{-6} for SO_2. These are orders of magnitude lower than those for cleaved $(10\bar{1}2)$ surfaces of Ti_2O_3 and V_2O_3,[1–3,5,6] whose surface cations have $3d^1$ and $3d^2$ configurations, respectively, and they are as low or lower than those for TiO_2 and $SrTiO_3$,[16–22] whose surface Ti cations are $3d^0$. In order to fully understand the inertness of the annealed α-Fe_2O_3(0001) surfaces, it would be necessary to know its geometric structure. An ideal cleaved surface should have the structure shown in Fig. 1 of Ref. 9, with its outermost atomic plane consisting of threefold-coordinated Fe ions. It is difficult to imagine that Fe ions that are missing one-half of their O ligands would not be significantly more active for chemisorption than the data presented here indicate. [On the other hand, it is somewhat surprising that the fourfold-coordinated Ti ions on the UHV-fractured TiO_2(001) surface have an electronic structure essentially the same as that for sixfold-coordinated bulk cations.[20]] The complex LEED patterns, which indicate an incommensurate overlayer structure, show that the actual surface geometry is more complicated than a simple truncation of the bulk lattice, but detailed I-V measurements and calculations for model structures would be necessary in order to determine a more realistic atomic arrangement.

The stable $3d^5$ electronic configuration of the Fe^{3+} cations in α-Fe_2O_3 lowers the energy of the $3d$ orbitals into the region of the O $2p$ band, resulting in the complicated valence-band structure shown in Figs. 1(b) and 1(c). The changes that occur in the valence-band structure as the surface stoichiometry is varied by sputtering and annealing suggest that the O $2p$ contribution to the valence band lies primarily in the upper portion of the band, with the cation contribution concentrated in the lower portion of the band. This is a qualitative conclusion, however, and further experiments utilizing a wider range of photon energies in order to separate p and d orbitals will be necessary before a more accurate identification of the origin of the various features in the band can be made. The measurements of Fujimori *et al.*,[11] although they utilized a wide range of photon energies, do not adequately address this problem due to the low resolution used. For example, they can only identify three components of the O $2p$/Fe $3d$ valence band, which they locate at 2.5, 5, and 7 eV below E_F; those energy locations differ by more than half an eV from those determined here (Table I).

There is strong evidence that the feature closest to E_F (at about 0.9 eV) in the UPS spectra is a cation-derived surface state. Upon exposure to O_2 it *completely* disappears (Fig. 3), and it almost completely disappears upon exposure to SO_2 (Fig. 10). If that feature had a bulk as well as a surface component, it would remain in the spectrum with reduced amplitude no matter what changes were produced in the electronic structure of the surface ions upon chemisorption. Adsorption of H_2O also partially depopulates the 0.9-eV peak, but H_2 chemisorption leaves it unchanged. (There is actually a slight increase in emission just below that peak after 10^5 L H_2 exposure in Fig. 8.)

The point defects that are created on α-Fe_2O_3(0001) by Ar^+ ion bombardment are qualitatively similar to those on other transition-metal-oxide surfaces.[12,21] Surface O^{2-} ions are preferentially removed, and in order to maintain

local charge neutrality the population of the $3d$ orbitals on the Fe cations adjacent to the defect is effectively increased, as evidenced by changes in the UPS spectra (Fig. 2) and the XPS spectra reported in Ref. 9. Since the atomic geometry of the annealed (0001) surface is not known, nothing can be said about the manner in which the additional electronic charge at defect sites is distributed.

The interaction of O_2 with α-Fe_2O_3(0001) is also qualitatively similar to its interaction with other transition-metal-oxide surfaces.[12,19,21] The sticking coefficient for O_2 on the well-ordered surface is very small, but the depopulation of the cation surface state and the increase in ϕ for large O_2 exposures indicate a negative adsorbed species. As is the case for Ti_2O_3 and V_2O_3,[1,3,5] the interaction between O_2 and the α-Fe_2O_3(0001) surface is complex, and the changes that occur in the shape of the valence band with O_2 exposure are too large to permit meaningful photoemission difference spectra to be obtained. Thus the adsorbed species cannot be identified in that way. Recent measurements of O_2 adsorption on NiO(100), however, gave strong evidence for an O_2^{2-} adsorbed species.[23] Superimposed on the changes in band shape is the usual movement of the valence band toward E_F as the surface cation orbitals are depopulated. This band movement is universal in transition-metal oxides, both for nearly perfect surfaces and for surfaces containing O-vacancy defects.[21] As for most other oxides, O_2 interacts strongly with O-vacancy surface defects, exhibiting a sticking coefficient close to unity. Owing to the complexity of the surface, however, nothing definitive can be said about the nature of the adsorbed species.

From the sequential difference spectra for H_2O adsorption on α-Fe_2O_3(0001), Fig. 6(b), it is apparent that more than one phase is adsorbing. The dominant features present up to 10^7 L are two peaks separated by about 5 eV. Such a two-peaked structure is characteristic of adsorbed OH^-, although the separation of the peaks is somewhat greater than that seen for OH^- on other oxides.[21] There are also other, weaker features in the difference spectra that could not be due to OH^-. These may arise from changes in the valence band, however, since it is rich in structure due to the overlapping O $2p$ and Fe $3d$ orbitals. The weak structure may in fact correspond to the transfer of charge out of cation orbitals to adsorbed OH^- radicals.

The difference spectrum obtained upon going from 10^7 to 10^8 L is qualitatively different than the two-peaked one seen at lower exposures. Its three-peaked structure is suggestive of molecularly adsorbed H_2O, but for exposures as large as 10^8 L impurities in the H_2O may have an effect. The primary impurity in the H_2O used in these experiments, as determined by mass-spectroscopic analysis in the UHV system, is O_2, with an upper limit of 500 ppm. Thus an exposure of 10^8 L H_2O could simultaneously expose the surface to 5×10^4 L of O_2, which could be sufficient to produce observable changes in the UPS spectra (see Fig. 3). Therefore no meaningful interpretation of the 10^8-10^7-L difference spectrum can be made.

The interaction of H_2O with the high-defect-density α-Fe_2O_3 surface, Fig. 7, is similar to that on the annealed surface in that the difference spectra are dominated by a two-peaked structure having nearly the same energies. We identify this as dissociative adsorption of H_2O, resulting in adsorbed OH^- radicals. A similar conclusion was drawn by Hendewerk *et al.*[10] from experiments on defective surfaces that were warmed through room temperature after H_2O had been condensed on them at 120 K. The main difference between the behavior of the sputtered and the annealed surfaces is that the two peaks begin to appear for as little as 0.5 L H_2O exposure of the sputtered surface.

The changes that are produced in the UPS spectra of α-Fe_2O_3(0001) upon exposure to H_2 are not understood. Gas-phase H_2 exhibits one broad peak in its UPS spectrum that would appear in Fig. 9 at 11.0 eV if the sample and gas-phase vacuum levels were aligned.[13] It thus seems unlikely that the broad peak at 6 eV corresponds to adsorbed H_2, since that would imply an extramolecular relaxation-polarization (ERPS) shift of 5 eV for H_2 upon adsorption, which seems unrealistically large. In addition, there is no reason to believe that H_2 would be a stable species adsorbed at room temperature; it is most likely to dissociate upon adsorption. It is possible that the broad peak in the difference spectra is an artifact resulting from the increase in the inelastic background emission increase? It is accompanied by only a slight increase in ϕ and no other major changes in the UPS spectra. An increased background emission could arise from scattering of electrons by a weakly adsorbed layer of molecules, but then one would also expect to see emission from the molecular orbitals of the adsorbate.

For H_2 exposures above 10^4 L, the 10.7-eV peak grows concurrently with a shoulder on the high-binding-energy side of the 6-eV peak. The peak at 10.7 eV is within 0.2 eV of the location of the 3σ peak for OH^- resulting from H_2O adsorption. The most probable interpretation is that H_2 dissociates and forms OH^- radicals with surface O^{2-} ions. The sticking coefficient for this process would then be about $10^{-4}-10^{-5}$. A possible cause of the increase in emission just below the 0.9-eV surface state when OH^- is formed is backdonation of charge from surface O^{2-} ions to adjacent cations.

The UPS spectra for the adsorption of SO_2 on α-Fe_2O_3(0001) provide evidence for a single, specific adsorbed phase (Figs. 10 and 11). The He I UPS spectrum for gas-phase SO_2 is included with the difference spectra in Fig. 11(b), with the combined $(5a_1+1b_1)$ orbitals[24] aligned with the highest-binding-energy peak in the spectra.[13] The resultant ERPS shift is 1.0 eV. Although the weak peak in the difference spectra near 7 eV aligns well with the combined $(1a_2+4b_2)$ orbitals of SO_2, the position of the lowest-binding-energy peak in the difference spectra does not agree at all with that of the gas-phase $6a_1$ orbital. Comparison of the data to XPS spectra for SO_3^{2-} ions in Li_2SO_3 gives no better agreement.[25] The spacing between the SO_3^{2-} $2a_1$ and the combined $(3a_1+2e)$ orbitals[24] is in agreement with that of the two higher-binding-energy peaks in Fig. 11(a), but the $3e$ and lower-binding-energy orbitals of SO_3^{2-} lie much farther from the $2a_1$ and $(3a_1+2e)$ orbitals than do the corresponding features in the UPS spectra of SO_2 on α-Fe_2O_3(0001). Relatively

good agreement with the UPS difference spectra is obtained for SO_4^{2-}, however, as shown in Fig. 11(c). The $2t_2$ orbital of SO_4^{2-} in $LiSO_4$ (Refs. 15 and 25) has been aligned with the 10.2-eV peak in Fig. 11(c). The spacings between the $2t_2$, the combined $(1e+3t_2)$ and the $1t_1$ orbitals of SO_4^{2-} are 3.5 and 2.3 eV,[15,26] respectively, compared to 3.1 and 2.0 eV for SO_2 on α-Fe_2O_3(0001). It is thus most probable that SO_2 coordinates to two surface O ions, resulting in an adsorbed complex similar to SO_4^{2-}. The small increase in work function and the depopulation of the cation surface state indicate that some electronic charge is transferred from surface cations to the adsorbed complex.

For a comparison of the chemisorption of SO_2 on transition-metal oxides and other materials, see the discussion in Sec. V B of Ref. 6.

IX. SUMMARY

Well-ordered, nearly stoichiometric α-Fe_2O_3(0001) surfaces produced by ion bombardment and annealing, which have been characterized previously using XPS and LEED,[9] have been studied by using ultraviolet photoemission spectroscopy. The valence band consists of overlapping O $2p$ and Fe $3d$ orbitals, giving rise to a complicated structure about 10 eV wide. Surface defects produced by Ar^+ ion bombardment consist primarily of oxygen vacancies, with a corresponding increase in the charge on surface cations. The nearly stoichiometric surface is quite inert to O_2, H_2O, H_2, and SO_2, and exposures greater than 10^3 L are necessary before any significant changes are apparent in the UPS spectra. The interaction of O_2 with the well-ordered surface changes the substrate band structure sufficiently that UPS difference spectra cannot be taken, and the adsorbed species cannot be identified. Work-function changes indicate only that it is negatively charged. The interaction of O_2 with surface defects is much stronger and results in oxidation of the reduced surface cations. H_2O dissociates upon adsorption on either the well-ordered or defect surface, giving rise to adsorbed OH^- ions. The changes that are produced in the UPS spectra of α-Fe_2O_3(0001) upon exposure to H_2 are not understood. The sticking coefficient of SO_2 on the well-ordered surface is less than 10^{-4}, but when it does stick it appears to bond primarily to surface O^{2-} ions, giving rise to an adsorption complex similar to the SO_4^{2-} ion, although UPS difference spectra do not give an unequivocal interpretation.

ACKNOWLEDGMENTS

The authors are pleased to acknowledge helpful discussions with Kevin Smith and Paul Dorain on the nuances of SO_2 chemisorption. The data for O_2 adsorption on the defect α-Fe_2O_3(0001) surface were taken by Mike Siegal. The α-Fe_2O_3 single crystals were kindly supplied by J. P. Remeika of AT&T Bell Laboratories. This work was partially supported by National Science Foundation (Solid State Chemistry Program) Grant No. DMR-82-02727.

*Present address: Surface Science Division, National Bureau of Standards, Gaithersburg, MD 20899.

[1]R. L. Kurtz and V. E. Henrich, Phys. Rev. B **25**, 3563 (1982).
[2]R. L. Kurtz and V. E. Henrich, Phys. Rev. B **26**, 6682 (1982).
[3]R. L. Kurtz and V. E. Henrich, Phys. Rev. B **28**, 6699 (1983).
[4]J. M. McKay and V. E. Henrich, Surf. Sci. **137**, 463 (1984).
[5]R. L. Kurtz and V. E. Henrich, J. Vac. Sci. Technol. A **2**, 842 (1984).
[6]K. E. Smith and V. E. Henrich, Phys. Rev. B **32**, 5384 (1985).
[7]J. H. Kennedy and M. Anderman, J. Electrochem. Soc. **130**, 848 (1983).
[8]G.-M. Schwab, Adv. Catal. **27**, 1 (1978).
[9]R. L. Kurtz and V. E. Henrich, Surf. Sci. **129**, 345 (1983).
[10]M. Hendewerk, M. Salmeron, and G. A. Somorjai, Surf. Sci. **172**, 544 (1986).
[11]A. Fujimori, M. Saeki, N. Kimizuka, M. Taniguchi, and S. Suga, Phys. Rev. B **34**, 7318 (1986).
[12]V. E. Henrich, Prog. Surf. Sci. **14**, 174 (1983).
[13]D. W. Turner, C. Baker, A. D. Baker, and C. R. Brundle, *Molecular Photoelectron Spectroscopy* (Wiley-Interscience, New York, 1970).
[14]J. A. Connor, M. Considine, I. H. Hillier, and D. Briggs, J. Electron Spectrosc. Relat. Phenom. **12**, 143 (1977).
[15]J. A. Connor, M. Considine, and I. H. Hillier, J. Chem. Soc., Faraday Trans. II **74**, 1285 (1978).
[16]V. E. Henrich, G. Dresselhaus, and H. J. Zeiger, Solid State Commun. **24**, 623 (1977).
[17]V. E. Henrich, G. Dresselhaus, and H. J. Zeiger, J. Vac. Sci. Technol. **15**, 534 (1978).
[18]V. E. Henrich, G. Dresselhaus, and H. J. Zeiger, Phys. Rev. B **17**, 4908 (1978).
[19]V. E. Henrich, Prog. Surf. Sci. **9**, 143 (1979).
[20]V. E. Henrich and R. L. Kurtz, Phys. Rev. B **23**, 6280 (1981).
[21]V. E. Henrich, Rep. Prog. Phys. **48**, 1481 (1985).
[22]G. Heiland and H. Luth, in *The Chemical Physics of Solid Surfaces and Heterogeneous Catalysis*, edited by D. A. King and D. P. Woodruff (Elsevier, Amsterdam, 1984), Vol. III.
[23]J. M. McKay and V. E. Henrich, Phys. Rev. B **32**, 6764 (1985).
[24]For SO_2, the molecular-orbital notation from Ref. 11 is used. For SO_3^{2-} and SO_4^{2-}, the notation of Ref. 23 is used.
[25]N. Kosuch, G. Welch, and A. Faessler, J. Electron Spectrosc. Relat. Phenom. **20**, 11 (1980).
[26]These spacings are taken from the He II UPS spectra in Ref. 13.